JOC The Journal of Organic Chemistry

Article

pubs.acs.org/joc

C2 Hydroxyl Group Governs the Difference in Hydrolysis Rates of Methyl-α-D-glycero-D-guloseptanoside and Methyl-β-D-glycero-D-guloseptanoside

Jeremy M. Beck,[†] Shawn M. Miller,[‡] Mark W. Peczuh,*[,‡] and Christopher M. Hadad*[,†]

[†]Department of Chemistry, The Ohio State University, 100 West 18th Avenue, Columbus, Ohio 43210, United States

[‡]Department of Chemistry, The University of Connecticut, 55 North Eagleville Road, Storrs, Connecticut 06269, United States

Supporting Information

ABSTRACT: A computational investigation into the hydrolysis of two methyl septanosides, methyl-α-D-glycero-D-guloseptanoside and methyl-β-D-glycero-D-guloseptanoside was undertaken. These septanosides were chosen as model compounds for comparison to methyl pyranosides and allowed direct comparison of α versus β hydrolysis rates for a specific septanoside isomer. Results suggest that hydrolysis takes place without proceeding through a transition state, an observation that was suggested in previous computational studies on exocyclic bond cleavage of carbohydrates. A conformational analysis of α- and β-anomers **1** and **2** and their corresponding oxocarbenium **3**, coupled with relaxed potential energy surface (PES) scans (M06-2X/6-311+G**, implicit methanol), indicated that hydrolysis of the α-anomer is favored by 1−2 kcal/mol over the β-anomer, consistent with experiment. Model systems revealed that the lowest energy conformations of the septanoside ring system destabilize the β-anomer by 2−3 kcal/mol relative to the α-anomer, and the addition of a single hydroxyl group at the C2-position on a minimal oxepane acetal can reproduce the PES for the septanoside **1**. These results suggest that the C2 hydroxyl plays a unique role in the hydrolysis mechanism, destabilizing the septanoside via its proximity to the anomeric carbon and also through its interaction with the departing methanol from the α-anomer via hydrogen-bonding interactions.

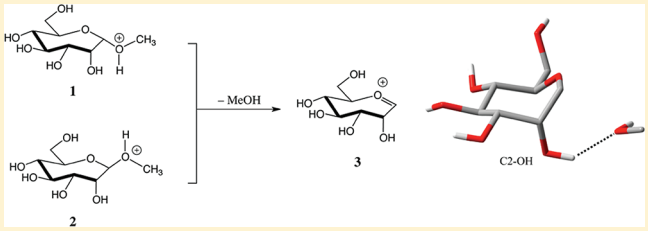

INTRODUCTION

The enzymatic hydrolysis of a glycosidic linkage is central to many important biological processes.[1] Moreover, mechanistic investigations of the reaction have spurred interest in the interplay between conformational geometry and orbital structure from a strictly chemical perspective.[2] The hydrolysis of acetals has therefore garnered broad interest from chemists and biochemists alike. Motivation for common interest in the reaction is amply illustrated in the case of retaining β-glycosyl hydrolases.[3] Distortion of the substrate's chair conformation to a sofa, or half-chair, conformation facilitates bond cleavage because the aglycone is appropriately positioned for departure based on stereoelectronics. That is, the sofa conformation aligns orbitals containing the lone pair electrons of the ring oxygen with the bond being cleaved en route to the oxocarbenium ion intermediate. This mechanism has support from structural and computational investigations.[4,5]

Research on the acid-catalyzed (chemical, non-enzymatic) hydrolysis of acetals has attempted to reconcile the fact that β-pyranosides have faster rates of hydrolysis compared to α-pyranosides, despite the better positioning of ring oxygen lone pair orbitals and breaking bonds in α-pyranosides (Table 1).[6] Depending on which molecules were used to address the question, the apparent discrepancy has been explained in terms of formation of an acyclic oxocarbenium for β-pyranosides (via cleavage of the ring oxygen−C1 bond instead of the aglycone oxygen−C1 bond) or in terms of differential low-energy conformations of the protonated glycosides. In the latter case, the protonated β-pyranosides (or model compounds) are higher in energy and along the reaction coordinate toward the oxocarbenium ion, whereas this is not the case for α-pyranosides. The consequence is that the activation energy for β-pyranosides is lower and the hydrolysis rate is therefore faster.

Table 1. Rate Constants for Glycoside Hydrolysis in 0.5 M HCl[a]

compound	T (°C)	10^{-5} k_{obs} (s^{-1})	ref
methyl glycero-guloside **1** (α)	50	11.4 ± 1.70	10
methyl glycero-guloside **2** (β)	50	5.38 ± 0.07	
methyl glucoside (α)	75	0.76	26
methyl glucoside (β)	75	1.46	26
methyl mannoside (α)	75	1.81	26
methyl mannoside (β)	75	4.34	26

[a]Hydrolysis experiments for **1** and **2** were conducted using DCl as acid.

Received: December 21, 2011
Published: April 11, 2012

Scheme 1. Hydrolysis of Methyl-α-D-glycero-D-guloseptanoside and Methyl-β-D-glycero-D-guloseptanoside[a]

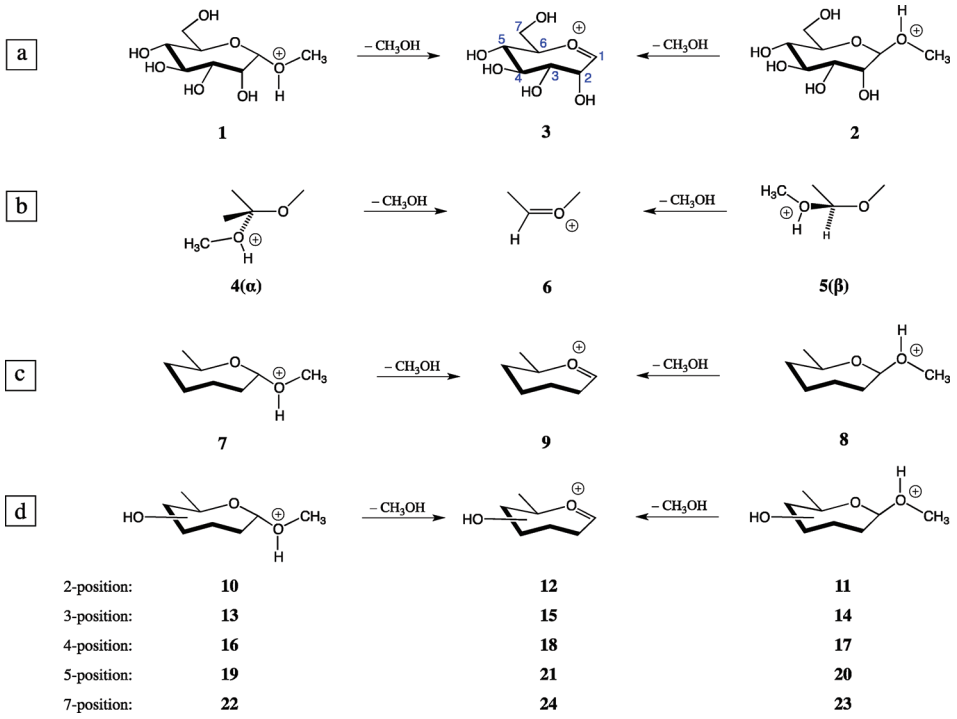

[a]Conditions: (a) Protonated methyl septanosides **1** and **2** and the product of methanol dissociation, oxocarbenium ion **3**. Note: Carbon numbering is shown on compound **3**. (b) Acyclic oxocarbenium model **6**, with its corresponding α and β analogues **4** and **5**. (c) Minimal oxepane acetals **7** and **8** and the product of methanol dissociation, oxocarbenium ion **9**. (d) Single hydroxyl-substituted acetals with their resulting oxocarbenium ions. Hydroxyl orientations on the ring are identical to compound **3**.

Due to the relationship between structure and reactivity of carbohydrates, the analysis of molecular configurations has been a focus of research. Recently, a peptidic probe was reported, capable of identifying the anomeric configuration of methyl D-galactopyranoside.[7] Capable of complexing the pyranosides in the gas phase, the peptide is able to determine the anomeric configurations without the influence of external factors. The probe, through vibrational spectroscopy, coupled with computational modeling, identified significant interactions between the oxygens at C1 and C2, which influenced the strength of the exo/endo-anomeric interactions. The authors concluded that re-evaluation of the influence of substituents at the C2-position was important to understanding reactivity and biological effects of sugars.

We are interested in the conformational profiles[8,9] and reactivity[10] of seven-membered ring carbohydrates called septanoses. The interest was motivated in part by the possibility that β-septanosides may be able to adopt distorted conformations in enzyme active sites with reduced energetic penalties relative to β-pyranosides. Incorporation of a nonhydrolyzable linkage into the design would then lead the way to inhibitors of retaining β-glycosidases. Toward that end, we undertook the characterization of hydrolysis rates of some model septanosides. We reasoned that the rates would give a preliminary read-out on the dynamics of the ring. Specifically, we wanted to know if septanosides would in fact have faster rates of hydrolysis compared to pyranosides. Additionally, we wanted to compare rates of hydrolysis for α- and β-anomers of the same septanoside. Reported here are hydrolysis rate constants for two methyl septanosides, methyl-α-D-glycero-D-guloseptanoside and methyl-β-D-glycero-D-guloseptanoside and a computational study that reproduces the key features that differentiate the hydrolysis rates of these two septanosides.

There have been several previous computational studies on glycoside hydrolysis, ranging from molecular mechanics modeling of the intermediate oxocarbenium ions[11] to ab initio modeling of the reaction pathways.[12,13] While Bowen et al. were able to locate transition states for hydrolysis of 2-methoxytetrahydropyrans,[11] their computational methods, taking place in the early 1990s, utilized gas-phase calculations at the HF/3-21G level of theory, considered to be insufficient by today's computational means. In a more recent study carried out by Deslongchamps et al., a relatively flat potential energy surface for both endo- and exocyclic cleavage for pyranosides was reported.[13] In fact, no transition state structures could be isolated for exocyclic hydrolysis at the HF/6-31G* level of theory in Deslongchamps' study, and so a C–O distance of 1.9 Å was chosen to compare relative energies at the bond-breaking "transition-state-like" structures between anomers. At these "transition state" structures, the energetic barriers were 4.6 and 5.3 kcal/mol for the α- and β-anomers, respectively, in good agreement with the experimentally observed 3:2 hydrolysis ratio in favor of the α-anomer of the reported tetrahydropyranal acetals.[14] It was also predicted that β-glycosides could only undergo exocyclic hydrolysis via a higher energy sofa conformation, a structure already beginning to resemble the resulting oxocarbenium ion.[13]

More recently, a series of studies involving molecular dynamics simulations on glycoside hydrolysis have been undertaken.[15–17] These simulations, using explicit solvent, depict the same two-step reaction described in previous computational studies: the first step was described as irreversible protonation of the exocyclic oxygen atom, and the

dx.doi.org/10.1021/jo202639g | J. Org. Chem. 2012, 77, 4242–4251

second was anomeric C−O bond cleavage. A recent study by Hünenberger also presents a new hypothesis for stereoselectivity, which is described as the *conformer and counterion distribution hypothesis*. In it, two conformational properties of the glycoside dictate stereoselectivity: (1) conformational preferences/steric interactions of the ring that modulate the accessibility of the anomeric carbon from either face, and (2) preferential coordination of a counterion on either face of the anomeric carbon, thereby promoting nucleophilic attack from the opposite face.[17] Their findings correlate well with the observed selectivity in a variety of solvents with several counterion activators, suggesting that conformational preferences do, in fact, play a distinct role in the glycosylation reactions. It is quite possible, therefore, that the same preferences should be evident in the reverse reaction, glycoside hydrolysis.

Another focus of study in glycoside hydrolysis has been the investigation of substituent effects on hydrolysis rates. Although there have been numerous studies on this topic, the general conclusion is that field effects caused by substituents have a large effect on the hydrolysis rate.[18] The ordering of field effects in six-membered ring systems is suggested to be 2-deoxy > 4-deoxy > 3-deoxy > 6-deoxy > parent,[19,20] with fluoride substitution being the opposite order, although the authors were careful to note that the experimental rates represent a milieu of products and mechanisms.[21] The rate of hydrolysis was observed to increase with the number of axial substituents, which was rationalized by steric 1,3 diaxial interactions that are ameliorated when forming the half-chair transition state.[22] However, substitution at the 2-hydroxyl substituent has been suggested to play a unique role in hydrolysis, in that it may aid in orienting incoming nucleophiles due to its proximity to the anomeric carbon.[23,24] It is important to note, however, that these findings[18] are based on analytical methods said to be more applicable to rigid ring systems,[25] whereas the pyranose and septanose rings are more flexible than the previously reported bicyclo systems. At the outset, it was therefore unclear what the effect of substituents would be on the reaction.

In this paper, we investigate the hydrolysis of methyl-α-D-glycero-D-guloseptanoside and methyl-β-D-glycero-D-guloseptanoside (**1** and **2**, respectively; see Scheme 1a) using computational methods to corroborate experimental observations. As the initial protonation step is a fast process, we focus our investigation on the slower step, C−O bond cleavage. Additionally, the effects of the ring system on hydrolysis will be investigated using a smaller oxocarbenium structure **6** (via compounds **4** and **5**; see Scheme 1b), while the effects of hydroxyl substituents on the ring will be investigated using a minimal oxepane acetal **7** (Scheme 1c), as well as by systematically adding hydroxyl groups to the ring system (Scheme 1d). In addition to single hydroxyl substitutions, as in Scheme 1d, substituent effects were also probed via the deletion of a single hydroxyl group from the parent acetal **1** or **2**. These structures are referred to as 2-deoxy, 3-deoxy, etc., reflecting the position from which the hydroxyl has been deleted.

RESULTS AND DISCUSSION

Determination of the Rate Constant for Hydrolysis of Methyl-β-D-glycero-D-guloseptanoside. We have reported on the hydrolysis of methyl α-septanosides derived from D-glucose, D-galactose, and D-mannose.[10] Determination of rate constants in that study used a series of ^{1}H integration values to quantify the concentration of the aglycon methyl group over time. Curve fitting of plots correlating the disappearance of methyl septanoside as a function of time gave k_{obs} values. In the original investigation, we determined the k_{obs} value for methyl-α-D-glycero-D-guloseptanoside **1** to be $1.14 \pm 0.17 \times 10^{-4}$ s^{-1}. Under the same assay conditions, the k_{obs} value for methyl-β-D-glycero-D-guloseptanoside **2** was determined to be $5.38 \pm 0.07 \times 10^{-5}$ s^{-1}. Table 1 collects the k_{obs} values for the two septanosides and also for the α- and β-anomers of methyl-D-glucoside and methyl-D-mannoside, respectively. The data indicate that methyl septanosides showed faster rates of hydrolysis under milder (based on temperature) hydrolysis conditions. Importantly, the ordering of anomers based on hydrolysis rate is switched for the septanosides in comparison to pyranosides; hydrolysis of α-septanoside **1** is roughly twice as fast as β-septanoside **2**, while hydrolysis of β-glucoside and β-mannoside are faster than their corresponding α-anomers.

Computational Methods. The conformational flexibility of simple seven-membered ring systems is well-known; however, our initial conformational analysis of unprotonated **2** showed that one ring conformation dominated (>90%) the Boltzmann distribution of conformers.[8] It was not obvious whether this stability would persist in the acidic conditions of the hydrolysis reaction. Therefore, the most favorable ring conformations of compounds for **1**, **2**, and **3** were studied by performing conformational searches on their nitrogen analogues **1a**, **2a**, and **3a** (Scheme 2). The nitrogen analogues were

Scheme 2. Septanoside Nitrogen Analogues Utilized for Molecular Mechanics Conformational Searches

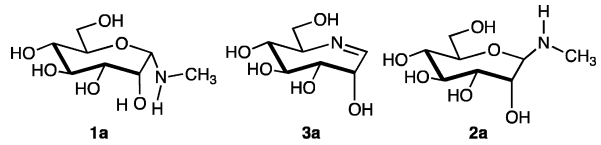

used in order to maintain a neutral charge state but similar valency and hybridization for each species. A stochastic conformational search was carried out in the Molecular Operating Environment suite of programs[27] using the MMFF94x force field,[28] with 10 000 iterations of the geometry and an energy cutoff of 10 kcal/mol. A subsequent geometry minimization ensured each structure was a stationary point on the potential energy surface. After replacing the nitrogen atoms with oxygens to regenerate the septanoside compounds, the resulting conformations were optimized in Gaussian 09[29] using the density functional B3LYP[30] with a 6-31+G** Pople-type basis set[31] with implicit solvation (methanol) using the polarizable continuum model[32] with atomic radii from the SMD method.[33] The combination of method and basis set was chosen due to its exhibited success in previous studies on septanoside conformational flexibility.[8]

Using the resulting B3LYP/6-31+G** optimized geometries of compounds **1** and **2**, transition state searches were carried out in Gaussian 09 to study the mechanism of exocyclic C−O bond cleavage to generate compound **3** and methanol. It should be noted that discrete transition states were located using the Hartree−Fock (HF) methodology for the potential energy surface (PES). However, energetics on the HF PES suggest that any inclusion of electron correlation eliminates any stability of the dissociated complex, resulting in the disappearance of the energetic barrier for bond cleavage, and subsequently the transition state, at higher levels of theory (see Supporting

dx.doi.org/10.1021/jo202639g | J. Org. Chem. 2012, 77, 4242−4251

Information). In the graphs, we have depicted a line for visual clarity of the asymptotic energy rise. Nevertheless, the potential energy surfaces for departure of methanol away from compounds **1** and **2** (derived from the lowest energy conformation of compound **3**) were calculated using the HF method with a 6-31+G** basis set in implicit methanol. Transition states were connected to their associated minima via intrinsic reaction coordinate[34] calculations. A vibrational frequency analysis confirmed each HF-optimized stationary point to be either a minimum or saddle point on the potential energy surface, and results were used for thermal and vibrational corrections to the free energy with frequencies scaled by a factor of 0.904.[35] HF potential energy surfaces are reported in the Supporting Information.

Due to a systematic failure in locating transition states using density functional theory (DFT) methods, as discussed in the previous literature,[12] relaxed PES scans were carried out by adding methanol to the anomeric carbon of compound **3**. Dissociation from both the α and β face of **3** was conducted by varying the anomeric C−O(methanol) distance from 1.4 to 4.4 Å in steps of 0.1 Å. Compound **3** was utilized as a starting point for these scans in order to eliminate perturbations in the relative energies of the resulting compounds **1** and **2** due to slight variations in hydrogen-bonding structure, in order to more fully investigate the differences between α and β bond cleavage.

In addition to the full septanoside structures, relaxed potential energy surface scans were carried out for departure of methanol to form a small oxocarbenium **6** (Scheme 1b), as well as oxepane acetal **9** formed by removing all hydroxyl groups from compounds **1** and **2**. Substituent effects at various ring positions on the potential energy surface were probed by adding a hydroxyl group to the relevant carbons (in the same relative orientation as the parent compound **1** or **2**; see Scheme 1d) and then re-performing the relaxed scan. A series of deoxy variants were calculated by deleting a single hydroxyl group from acetals **1** or **2** and re-performing relaxed scans.

Refined energies were generated using the M06-2X density functional[36] with a 6-311+G** basis set. The M06-2X functional is an adaptation of the M05-2X functional[37] which, in combination with the aforementioned basis set, has recently been shown to be one of the most successful methods for accurately generating conformational energetics in carbohydrate systems due to its incorporation of mid-range correlative effects.[38] MP2 single-point energy calculations were also performed, and these mimic the trends of the M06-2X calculations. However, dissociation energies are consistently 2 kcal/mol lower than the DFT methods. The MP2 values are presented in the Supporting Information.

Conformational Flexibility of Compounds 1 and 2. Following the conformational search protocol described previously, a total of 72 unique conformations were located for compound **1**, while 98 were located for compound **2**. Of these conformations, the twisted chair form dominates the conformational landscape for both compounds **1** and **2**. The lowest energy conformation for compound **1** was the $^{3,4}TC_{5,6}$ conformer (Figure 1). However, a total of 54 conformers lie within 7.5 kcal/mol of the lowest energy conformation of compound **1**; the largest contributing conformations are $^{3,4}TC_{5,6}$ (25 structures) and $^{1,2}TC_{3,4}$ (14 structures); see the Supporting Information for a full list of the conformations. Even with a fairly diverse set of conformations, however, the $^{3,4}TC_{5,6}$ structure dominates the lowest energy structures,

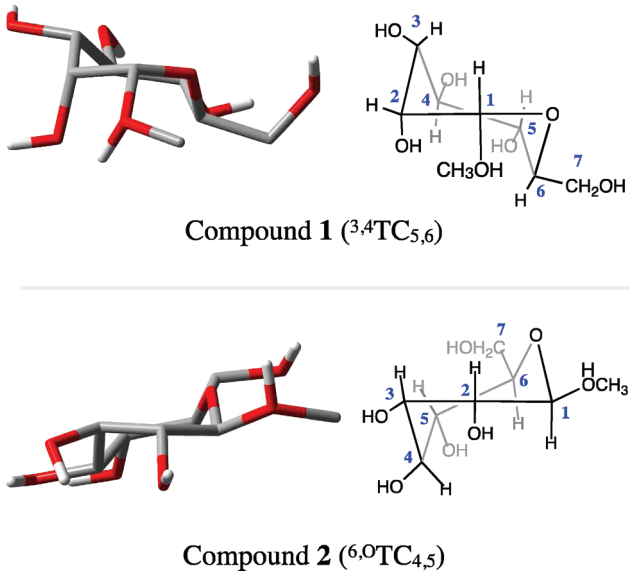

Figure 1. Lowest energy conformations of compounds **1** and **2** determined at the B3LYP/6-31+G** level of theory with consideration of implicit methanol solvation (SMD). For a full listing of the conformations of compounds **1** and **2**, see the Supporting Information.

consistent with a similar septanoside investigation reported previously.[8] The $^{1,2}TC_{3,4}$ structures of compound **1** predominate at the higher 6−7.5 kcal/mol end of the energy scale.

The conformational landscape of compound **2** is much less diverse than compound **1**. A total of 33 structures were found to be within 7.5 kcal/mol of the lowest energy for this structure. The most favorable structure of compound **2**, which was 3.4 kcal/mol higher in energy than compound **1**, is represented by two degenerate conformations: $^{6,O}TC_{4,5}$ and the same $^{3,4}TC_{5,6}$ conformer located for compound **1** (Figure 1). However, unlike the conformational landscape of compound **1**, the $^{6,O}TC_{4,5}$ conformation was found to dominate the conformational distribution, with 19 of the 30 lowest energy conformers being the $^{6,O}TC_{4,5}$ conformer (see Supporting Information). These findings are consistent with previous conformational evaluations on (unprotonated) **2**.[8]

Conformational Flexibility of Compound 3. Compound **3**, unlike compounds **1** and **2**, is significantly restricted in its conformational flexibility by the presence of the ring's double bond. Only nine conformations were located, and it is clear from these results that the chair conformation ($^{1,O}C_4$) dominates the conformational distribution (Figure 2). For the $^{1,O}C_4$ conformation, rotamers of the C6−C7 bond as well as slight variations and direction in the hydrogen-bonding pattern around the ring contribute to the smaller changes in energy. While two of the nine conformations (**3**−**6**, **3**−**7**) adopt a half-chair conformation ($^3H_5$), they are two of the highest energy conformers located, with relative energies at 4.3 and 3.3 kcal/mol, respectively.

Relaxed Potential Energy Surface Scans. Conformers **3**−**1**, **3**−**2**, **3**−**3**, and **3**−**7** were selected for relaxed potential energy surface scans in order to study both the effect of the C6−C7 rotamers and hydrogen-bonding patterns on the hydrolysis of compounds **1** and **2**. Although **3**−**4** is only slightly higher in energy than **3**−**3**, there are no unique structural features that distinguish it from **3**−**1** and **3**−**2**, and therefore, it was omitted. Scans were performed on **3**−**7** to account for the half-chair ring conformation in the potential

dx.doi.org/10.1021/jo202639g | J. Org. Chem. 2012, 77, 4242−4251

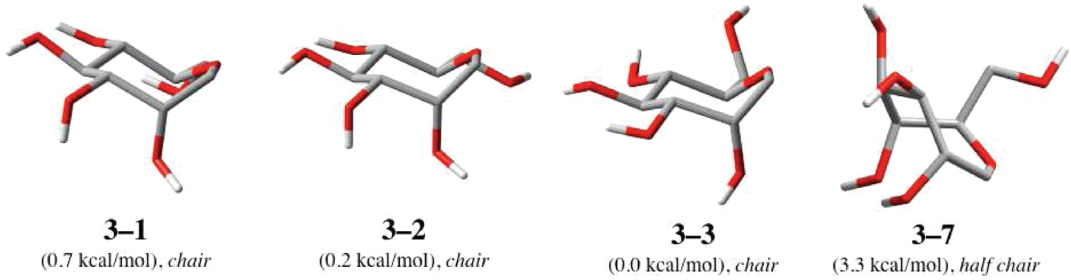

Figure 2. Selected conformations of compound **3**, with ring conformation and relative energies. For a list of geometries and names of all conformations of compound **3**, refer to the Supporting Information.

energy surface for loss of methanol. While scans were performed on **3**−**2**, the corresponding compound **2** (*β*-anomer) was optimized with the hydrogen at C1 adopting an axial orientation, which was unable to interconvert to the equatorial position after methanol dissociation. This axial orientation resulted in a significant ring distortion, causing the ring to open and re-form as a six-membered ring system, and as such, the results will not be presented in the main body of the text (see Supporting Information for more information).

Oxocarbenium ***3***−***3***. The potential energy surfaces for methanol dissociation to form **3**−**3** from both *α* and *β* faces are presented in Figure 3. Methanol as an implicit solvent (SMD)

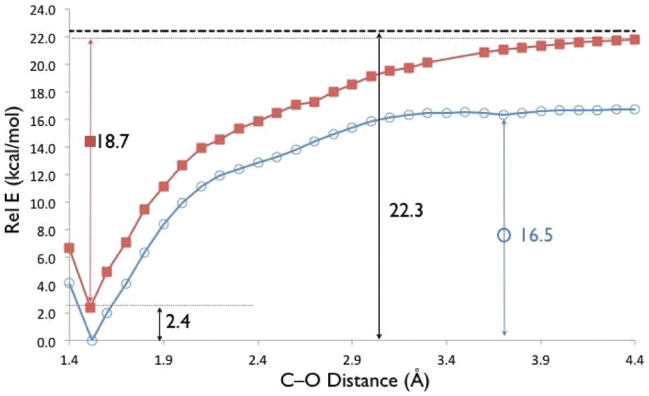

Figure 3. Potential energy surface for the hydrolysis of *α*-anomers (open circles, ○) and *β*-anomers (closed squares, ■) derived from compound **3**−**3**. Energies are determined at the M06-2X/6-311+G**//B3LYP/6-31+G** level of theory using SMD−methanol for both single-point energies and the geometry optimization. The missing points for the *β*-anomer at 3.4−3.5 Å are caused by a systematic failure in the SCRF routine when defining the solute cavity. The black dashed line represents the energy of infinitely separated **3** and methanol.

was used in the calculations. For departure from the *α* face, a minimum in energy was observed at a C−O distance of 1.52 Å. An asymptotic barrier of 16.5 kcal/mol is associated with loss of methanol, which is consistent with the previously observed lack of transition state geometries, as well as our own lack of success in isolating transition states using DFT methods. The energy for infinitely separated **3** and methanol lies 22.3 kcal/mol higher in energy than compound **1** and roughly 5.8 kcal/mol higher in energy than the dissociated complex. The PES for loss of methanol along the *β* face also possesses a minimum at 1.51 Å, although it is higher in energy than the *α* face departure by 2.4 kcal/mol. The energetic barrier for loss of methanol from the *β* face is also slightly higher, at 18.7 kcal/mol. As can be seen in Figure 3, the dissociated complex for *β* departure will be isoenergetic with the infinitely separated products. The presence of the stabilized product complex for departure from the *α*-anomer results in a 2.2 kcal/mol thermodynamic preference for the hydrolysis of the *α*-anomer. The only major structural difference between the two dissociated complexes is the presence of a hydrogen bond between the C2 hydroxyl group and the departing methanol from the *α* face. In the dominant conformations of the septanoside system, there are no such interactions for *β* face departure, as there are no accessible hydroxyl groups on that face of the ring. Additionally, the C7 hydroxyl group is distant enough that a hydrogen bond is not feasible at shorter bond distances (see Figure 4). If simply comparing compounds **1** and **2** relative to infinitely separated **3**+MeOH, this interaction with the C2 hydroxyl group would be missed and the calculations would predict that *β* departure would be preferred, contradicting our experimental findings. Comparison of the energetics relative to the infinitely separated products, as well as to the interacting product complexes for the remainder of the conformations, is reported in the Supporting Information.

Oxocarbenium ***3***−***1***. The dissociation of methanol from **3**−**1** bears a strong resemblance to the PES for **3**−**3**, which is unsurprising given that the major difference between the two conformers is a 120° rotation of the C6−C7 bond (Figure 5). The asymptotic barrier for loss of methanol is increased slightly to 17.5 kcal/mol, while the energy gap is still roughly 2.4 kcal/mol between the two anomers. Dissociation from the *α* face of **3**−**1** also benefits from a hydrogen bond between the C2 hydroxyl group and the methanol at a C−O distance of roughly 2.5 Å. In **3**−**1**, the C7 hydroxyl group is oriented away from the departing methanol of the *β* face (see conformation in Figure 2), but comparable energetics between conformers **3**−**1** and **3**−**3** suggest this rotation has little or no effect on the PES for dissociation of methanol.

Oxocarbenium ***3***−***7***. Compound **3**−**7**, being a unique half-chair conformation, exhibits a markedly different PES than those observed for conformers **3**−**1** and **3**−**3**. For the equilibrium geometry of the *α*-anomer, the methanol unit forms a hydrogen bond with the C5 hydroxyl group. This interaction deforms the ring to resemble a twisted boat conformation, and the methanol hydrogen is mostly dissociated from methanol (O−H distance: 1.3 Å) to interact with the C5 hydroxyl oxygen (H−O distance: 1.1 Å). This dissociation corresponds to a decrease of the methanol−ring O−C1 bond to 1.43 Å at the minimum energy structure. For departure from the *β* face, the methanol unit does not form any hydrogen-bonding interactions, and the ring system maintains its original half-chair conformation. Thus, for the dissociation of methanol from the *α* and *β* faces of **3**−**7**, two different conformations of

dx.doi.org/10.1021/jo202639g | J. Org. Chem. 2012, 77, 4242−4251

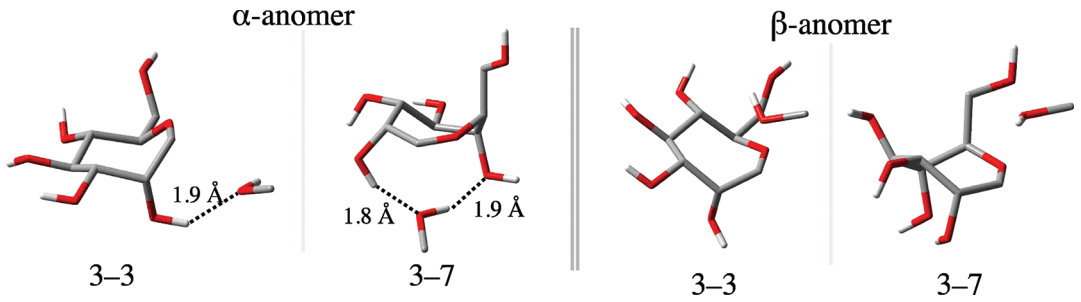

Figure 4. Products of methanol dissociation from the α- and β-anomers of compounds **3**–**3** (identical to **3**–**1**) and **3**–**7** at a C–O distance of 2.6 Å. The C2 hydroxyl group donates a hydrogen bond to the departing methanol for the α-anomer, while a lack of hydroxyl to interact with the β-anomer causes the methanol to depart directly above the ring.

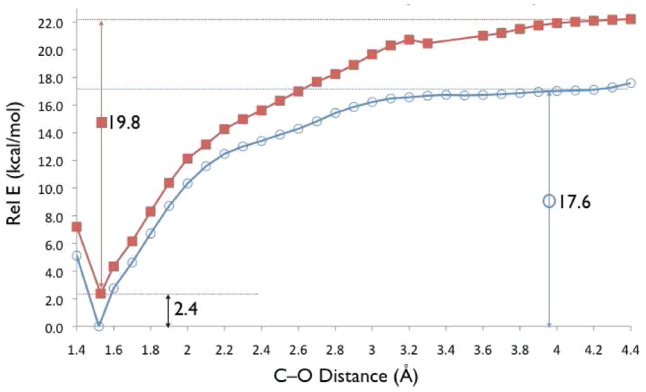

Figure 5. Potential energy surface for the hydrolysis of α-anomers (open circles, ○) and β-anomers (closed squares, ■) derived from conformer **3**–**1**. Energies are determined at the M06-2X/6-311+G**//B3LYP/6-31+G** level of theory using implicit consideration of methanol (SMD) for both single-point energies and complete geometry optimization. The missing points for the β-anomer at 3.4–3.5 Å are caused by a systematic failure in the SCRF routine when defining the solute cavity.

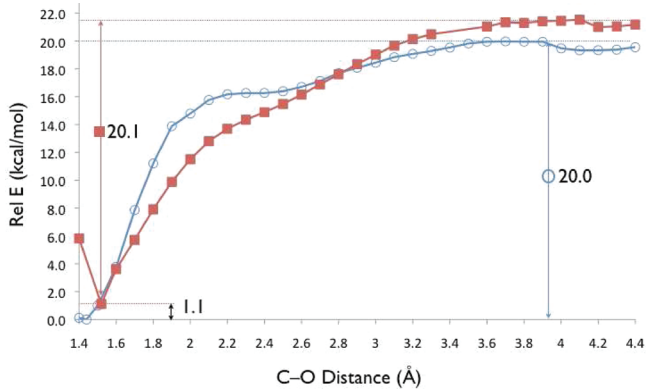

Figure 6. Potential energy surface for the hydrolysis of α-anomers (open circles, ○) and β-anomers (closed squares, ■) derived from compound **3**–**7**. Energies are determined at the M06-2X/6-311+G**//B3LYP/6-31+G** level of theory using implicit methanol solvation (SMD) for both single-point energies and the geometry optimization. The missing points for the β-anomer at 3.4–3.5 Å are caused by a systematic failure in the SCRF routine when defining the solute cavity.

the ring system are being compared, and the minimum in energy for the α face departure corresponds to a methoxy unit bonded to the ring more than a methanol unit. This is indicated by the lack of any real energetic gap between the anomers at a C1–O distance of 1.5 Å (Figure 6); the twisted boat conformation most likely overrides any energetic preference of the α face departure in the half-chair conformation. The only energy gap observed at the equilibrium structures more likely corresponds to sharing of the dissociated proton between methanol and the C5 hydroxyl group. Due to this strong methanol/C5 hydroxyl interaction, as the methanol dissociates from the α face, a hydrogen-bonding bridge is formed, with the C2 hydroxyl acting as a hydrogen bond donor to the methanol and the methanol donating to the C5 hydroxyl (Figure 4). This is in contrast to the single hydrogen bond formed for the other conformers, which corresponds to the methanol accepting a hydrogen bond from the C2 hydroxyl and moving around the edge of the ring, rather than over its face (Figure 4). Even so, dissociation of methanol from the α face (ΔE = 20.0 kcal/mol) and the β face (ΔE = 20.1 kcal/mol) is essentially equivalent for **3**–**7**. For clarity, we have elected to compare energetics for the α-anomer at 1.5 Å, as the methanol proton is no longer partly dissociated, and the relative energies should be more indicative of the desired C1 methanol reactants. The dissociation energy of the α-anomer is 1.1 kcal/mol lower in energy than the β-anomer, as estimated by the energetic differences between a C–O distance of 1.5 Å and the dissociated complexes (Figure 6).

Septanoside System Conclusions. From the results presented above, it is clear that there is a thermodynamic preference for dissociation of methanol from the α face of the septanoside ring, which is consistent with experimental observations. In the chair conformation, there is roughly a 2 kcal/mol energy gap in favor of the α face departure over the β face departure. This preference is also observed in the conformational searches on compounds **1** (α) and **2** (β), suggesting that starting from conformations of compound **3** is a reasonable choice. The calculated preference for dissociation of methanol from the α face is also consistent with our experimentally observed 2:1 (α/β) ratio of hydrolysis rate constants (Table 1). However, the data do not make clear which features give rise to this preference; the only consistent interaction between conformations along the potential energy surface is the formation of a hydrogen bond at a C–O distance of roughly 2.5 Å for the α face departure, with the C2 hydroxyl acting as either a hydrogen bond donor (**3**–**3**) or acceptor (**3**–**1**) with the departing methanol. We hypothesized that the components of the dissociation energy could be elucidated through the use of smaller model systems to build up to the full septanoside system, and we will describe our efforts toward this goal in the following sections.

dx.doi.org/10.1021/jo202639g | J. Org. Chem. 2012, 77, 4242–4251

Hydrolysis via Oxocarbenium ions 6 and 9. In order to decompose the contributions to the dissociation energies for loss of methanol from compounds **1** (α) and **2** (β), relaxed potential energy surface scans were carried out via a small acyclic oxocarbenium ion **6** as well as via a minimial cyclic oxocarbenium ion **9** (Scheme 1). These potential energy surfaces are presented in Figure 7. Both systems possess

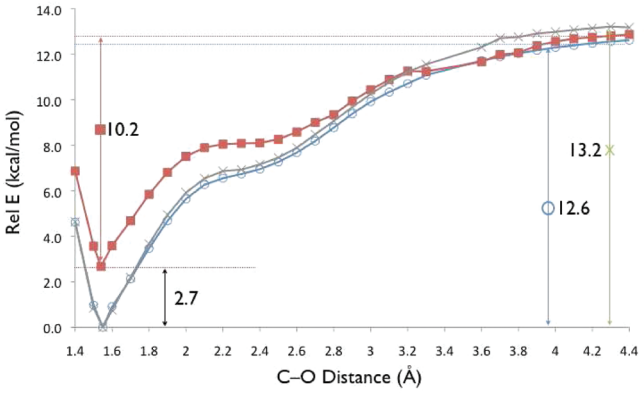

Figure 7. Potential energy surface for the hydrolysis of compounds **7** (α, open circles, ○) and **8** (β, closed squares, ■), as well as the small oxocarbenium ion (x's, pathways for **4** and **5** were found to be identical). Energies are determined at the M06-2X/6-311+G**//B3LYP/6-31+G** level of theory using SMD–methanol for both single-point energies and the geometry optimization.

dissociation energies much lower than the full septanoside system, suggesting that addition of the ring system does not perturb the dissociation energy to any great extent relative to acyclic oxocarbenium **6**. However, the β analogue of the minimal oxepane (**8**) is destabilized by 2.7 kcal/mol relative to the α analogue (**7**) at their equilbrium geometries, which is also observed in the fully hydroxylated septanoside chair conformation (Figure 3 and Figure 5) and is of roughly the same magnitude. This suggests that destabilization of the β-anomer relative to the α-anomer can be attributed to the ring system rather than the presence of substituents on the ring, although substituents may play a large role in increasing the dissociation energy of methanol.

Exoanomeric Effects. While the potential energy surfaces presented above represent the lowest dissociation energy trajectories for compounds **1** and **2**, the equilibrium structures associated with **1** feature methanol in an anti-orientation with regard to the ring oxygen. However, the exo-anomeric effect suggests that methanol should prefer the gauche orientation.[39] A second set of calculations which placed methanol in the gauche orientation revealed that the dissociation energy increases significantly for departure from the α face, up to 22.8 kcal/mol. This increase is brought about by energy shifts on both ends of the potential energy surface. First, the equilibrium complex is slightly more stable (1.9 kcal/mol). Next, the exocyclic C–O bond decreases in length from 1.510 Å in the anti-orientation to 1.496 Å in the gauche orientation. However, the bulk of the shift in dissociation energy is due to a destabilization of the dissociated complex by 4.1 kcal/mol (Figure 8).

A further analysis of the HF-optimized potential energy surfaces for the two orientations of methanol revealed that, while the equilibrium structure of the gauche orientation is more stable, the transition state structure for gauche is higher in

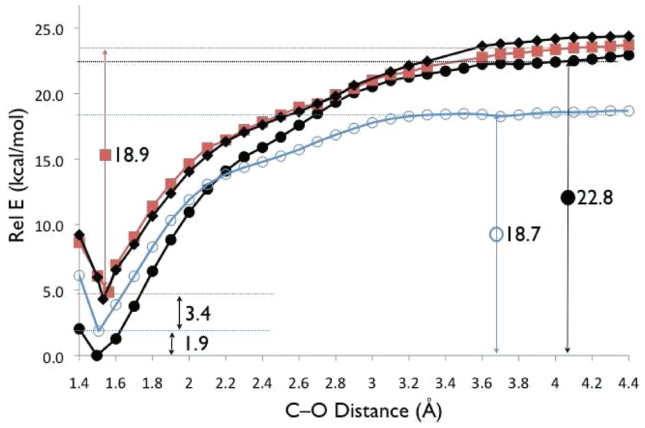

Figure 8. Potential energy surface for the hydrolysis of **1** (α; anti, open circles ○, gauche, closed circles ●) and **2** (β; gauche, closed squares ■, anti, closed diamonds ♦) analogues of the parent septanoside conformer **3**–**3**. Energies are determined at the M06-2X/6-311+G**//B3LYP/6-31+G** level of theory using SMD–methanol for both single-point energies and the geometry optimization.

energy than that for the anti-orientation (see Supporting Information). This change in orientation is determined to have little to no effect on dissociation of methanol from the β face (Figure 8). Optimizations carried out using the HF methodology indicate a barrier of roughly 3 kcal/mol for interchange between the anti and gauche orientations, suggesting that the two orientations of methanol could rapidly equilibrate (see Supporting Information).

Substituent Effects on Hydrolysis. The effect of substituents on glycoside hydrolysis rates is well-known, and it has been observed that deoxygenation generally increases the rate of hydrolysis.[18] The effect of hydroxylation at each position on the septanoside ring (see Scheme 1 for nomenclature and numbering) was studied via the addition of hydroxyl groups onto **7** or **8** and a recalculation of the relaxed potential energy surface scans. Deoxy species were investigated by removing a single hydroxyl group from compounds **1** and **2** and performing relaxed PES scans. The parent compound **3**–**3** was utilized to study substituent effects as that structure represents the lowest energy conformation of the septanoside.

Hydroxylation at the C2-position gives compounds **10**–**12**. The dissociation energy for methanol departure from the α face (**10**) increases to 18.9 kcal/mol, roughly equivalent to the dissociation energy from the fully hydroxylated septanoside structure (compound **1**, ~17 kcal/mol). In order to determine whether the change in dissociation energy was due to electronic effects or hydrogen bonding, the C2 hydroxyl was modified to a fluoride. The resulting PES suggests that electronic effects are the main driving force at shorter bond distances (1.5–2.6 Å), whereas at longer bond distances, the OH group acts as a hydrogen bond donor, as evidenced by the 2.5 kcal/mol reduction in energy when compared to fluoride (Figure 9). Departure from the β face in **11** encounters a dissociation energy of 14.4 kcal/mol when a hydroxyl group occupies C2. This falls much closer to bare ring **8** than the hydroxylated ring **2**. The dissociation energy is reduced to 12.6 kcal/mol for the fluoro analogue. Single-point energies following modification of the hydroxyl group back to hydrogen reproduce the PES for dissociation from the unsubstituted oxepane acetal **9** (Figure 7), indicating that observed differences in the PES can be

dx.doi.org/10.1021/jo202639g | J. Org. Chem. 2012, 77, 4242–4251

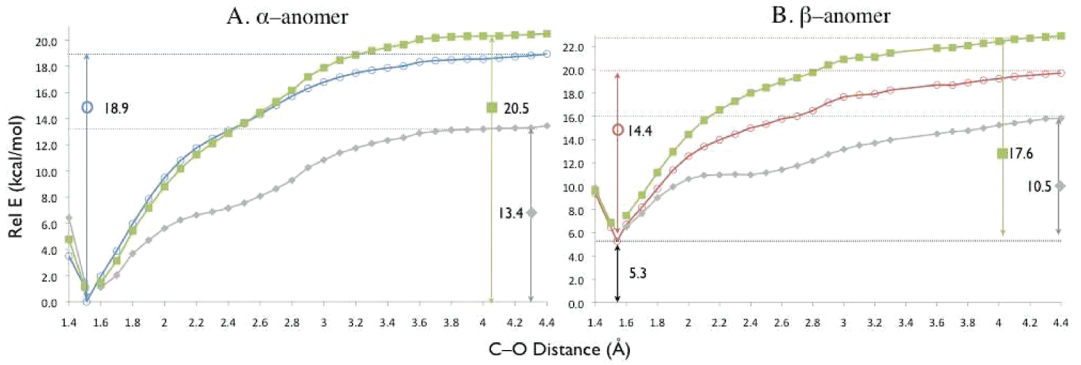

Figure 9. Effect of substituting a hydroxyl group (open circles, ○) and fluoride (closed squares, ■) at the C2-position on the dissociation of methanol for the α (A) and β (B) analogues. Substituting hydrogen (closed diamonds, ♦) regenerates the potential energy surface for dissociation of methanol from a bare septanoside ring. Energies are determined at the M06-2X/6-311+G**//B3LYP/6-31+G** level of theory using implicit methanol solvation (SMD) for both single-point energies and the geometry optimization.

attributed to the substituents on the ring, rather than simply a change in methanol orientation relative to the ring.

Using an identical set of calculations, the effect of hydroxylation at the other ring positions on the PES for dissociation of methanol from the oxocarbenium ion was investigated (Table 2). From these results, it is apparent that the C2-position does, in fact, have the largest role on perturbation of the dissociation energies for departure from both faces. However, no single hydroxyl substitution can reproduce the predicted dissociation energy for the β face departure. Each of the remaining positions on the ring have remarkably similar perturbations in regard to individual hydroxyl units. At most, the dissociation energy is altered by 2 kcal/mol relative to **7** and **8**.

Table 2. Effect of Hydroxyl Positions on Equilibrium Geometry Energy (ΔE_{eq}) and Dissociation Energy for Loss of Methanol (ΔE) from the α- and β-Anomers of Septanoside Compound 7[a]

	ΔE_{eq} (β–α)	ΔE (α)	ΔE (β)
9	2.7	12.6	10.2
12	5.3	18.9	14.4
15	3.4	14.3	10.0
18	2.9	13.7	11.1
21	4.6	14.7	10.8
24	2.5	14.1	11.7
2-deoxy (**3**–**3**)	2.8	17.6	14.8
3-deoxy (**3**–**3**)	3.0	16.0	17.3
4-deoxy (**3**–**3**)	3.2	16.2	17.4
5-deoxy (**3**–**3**)	1.3	14.4	17.2
7-deoxy (**3**–**3**)	3.8	16.3	17.4
3–**3** (parent)	2.4	17.6	19.8

[a]Energies (kcal/mol) are determined at the M06-2X/6-311+G**//B3LYP/6-31+G** level of theory in implicit (SMD) solvation for methanol. The C3-, C4-, and C5-OH groups are in equatorial positions, while the C2-OH is in an axial position. These orientations are adopted to be representative of the parent compound, **3**–**3**.

A series of potential energy surfaces for the deoxy analogues (removing a single hydroxyl group from **3**–**3**) were investigated (Table 2). In these scans, the calculated dissociation energies range from 14.4 to 19.8 kcal/mol, with the majority of systems being between 16–18 kcal/mol. Two deoxy systems exhibit significantly altered energetics: 2-deoxy (17.6 kcal/mol, α hydrolysis; 14.8 kcal/mol, β hydrolysis) and 5-deoxy (14.4 kcal/mol, α hydrolysis). Relative dissociation energies mirror the single hydroxyl substituent effects (Table 3). The elimination of the 2-hydroxyl lowers the dissociation energy significantly. Alteration at any other position has a moderate but consistent perturbation of roughly 2–3 kcal/mol on the dissociation energy. Interestingly, the 2-deoxy alteration is the only alteration in which the infinitely separated and product complex energetics predict that β departure would be preferred (Tables 2 and 3).

Table 3. Dissociation Energies (kcal/mol) of Compound 3–3 and Its Deoxy Analogues, Relative to Infinitely Separated Products[a]

	ΔE (α)	ΔE (β)
2-deoxy (**3**–**3**)	17.2	14.4
3-deoxy (**3**–**3**)	20.0	17.0
4-deoxy (**3**–**3**)	20.4	17.2
5-deoxy (**3**–**3**)	19.1	17.8
7-deoxy (**3**–**3**)	21.0	17.2
3–**3** (parent)	23.3	20.8

[a]PES calculated at the M06-2X/6-311+G**//B3LYP/6-31+G** level of theory in SMD–methanol. All points calculated for the PES are reported in the Supporting Information. Structures for the deoxy analogues are derived from compound **3**–**3**.

It is clear that altering the substituent at the 2-position exhibits consistently different behavior than other ring positions, mainly owing to its proximity to the anomeric carbon and departing methanol, as well as 2,4- and 2,6-diaxial interactions between the 2-OH and protons on the 4- and 6-positions. These interactions are evident by slight geometric perturbations around the anomeric carbon and endocyclic oxygen. The bond between C1 and the departing methanol is only slightly longer (0.01 Å) for the 2-deoxy species, although the methanol is rotated 15° due to loss of the steric clashes with the 2-OH group. In addition, the torsional angle around the C1–O(methanol) bond is increased relative to the other deoxy compounds. These geometric perturbations and the calculated energetics suggest that the 2-hydroxyl group destabilizes the septanoside compound relative to hydrogen by altering the orientation around the forming oxocarbenium ion double bond. This is evident when comparing relative energies of the differentially hydroxylated septanosides, where the C2 hydroxyl

dx.doi.org/10.1021/jo202639g | J. Org. Chem. 2012, 77, 4242–4251

is the highest in energy relative to other positions, and the 2-deoxy species is the lowest in energy relative to the other deoxy variants.

CONCLUSIONS

Methyl septanoside hydrolysis has been modeled using density functional methods. Relaxed potential energy surface scans at various levels of theory suggest that a discrete transition state for dissociation of methanol does not exist using DFT methodologies, which is consistent with several previous ab initio studies on glycoside hydrolysis. When comparing septanosides to pyranosides, the experimental and computational results clearly indicate that hydrolysis of septanosides occurs at a faster rate than pyranosides and under milder conditions. The implication drawn from this is that the seven-membered ring septanoside is, in fact, more flexible than a pyranoside ring. Initial impressions would suggest that, due to the high structural similarity between oxocarbeniums of the six- and seven-membered rings, mimicry of the half-chair/sofa β-pyranosides may be possible in a glycosidase active site.

Comparison of α- and β-septanoside hydrolysis led to the following conclusions. Calculations predict that the α face departure of methanol as in **1** encounters a dissociation energy of roughly 17−18 kcal/mol, while β face departure as in **2** possesses a dissociation energy that is roughly 1−2 kcal/mol higher in energy. Although exo-anomeric effects cause the gauche orientation of methanol to be preferred by roughly 2 kcal/mol over the anti-orientation for **1**, dissociation of methanol from the gauche orientation is predicted to encounter a significantly larger barrier (22.8 kca/mol) due to destabilization of the dissociated complex. However, an interchange of orientations is predicted to possess a low barrier (3 kcal/mol), suggesting that the two orientations can rapidly interconvert. Calculations involving model systems indicate several perturbations caused by the ring system on the hydrolysis pathway. First, the presence of the ring system results in an inherent destabilization, raising the energy of the β face departure by roughly 2.5 kcal/mol over the α face departure. Second, the presence of hydroxyl groups at each position on the septanose ring have varying degrees of effect on dissociation energy for methanol, a phenomenon observed previously for pyranoses/furanoses. Specifically, it was found that the C2 hydroxyl, which plays a role in directing the dissociated methanol from the α-anomer around the edge of the ring, raises the dissocation energy from 12 to 18 kcal/mol, single-handedly accounting for the dissociation energy of methanol from α-septanoside **1**. No other single hydroxyl substitution was calculated to have a perturbation larger than 2 kcal/mol on the dissociation energy. A series of calculations on the deoxy analogues indicated a similar contribution of the 2-position to the overall dissociation energy. Removal of the C2 hydroxyl lowers the dissociation energy significantly. The proximity of the axial C2 hydroxyl to the anomeric carbon produces small geometric perturbations around the endocyclic ring oxygen that raises the overall dissociation energy for the loss of methanol to a significantly higher degree than any other position. These results, in combination with the observation that substituent effects are more muted at each of the other positions, suggest that the hydroxyl at the C2-position plays a unique role in the hydrolysis pathway.

ASSOCIATED CONTENT

Supporting Information

Kinetics data from hydrolysis experiments on **2**, potential energy surface scan energies and Cartesian coordinates, HF-determined transistion state structures and associated minima for compounds **3** and **4**, and conformational energetics and assignments. This material is available free of charge via the Internet at http://pubs.acs.org.

AUTHOR INFORMATION

Corresponding Author

*E-mail: mark.peczuh@uconn.edu, hadad.1@osu.edu.

Notes

The authors declare no competing financial interest.

ACKNOWLEDGMENTS

The authors would like to acknowledge the Ohio Supercomputer Center for a generous grant of computational resources. M.W.P. thanks NSF for a CAREER award (CHE-0546311). S.M.M. was the recipient of a UConn Summer Undergraduate Research Fellowship (SURF).

REFERENCES

(1) (a) Freeze, H. Degradation and Turnover of Glycans. In *Essentials of Glycobiology*; Varki, A., Cummings, R., Esko, J., Freeze, H., Hart, G., Marth, J., Eds.; Cold Spring Harbor Laboratory Press: Cold Spring Harbor, NY, 1999; pp 267−284. (b) http://www.cazy.org/. (c) Cantarel, B. L.; Coutinho, P. M.; Rancurel, C.; Bernard, T.; Lombard, V.; Henrissat, B. *Nucleic Acids Res.* **2009**, *37*, D233−D238. (d) Davies, G.; Henrissat, B. *Structure* **1995**, *3*, 853−859.

(2) Kirby, A. J. *Acc. Chem. Res.* **1984**, *17*, 305−311.

(3) Heightman, T. D.; Vasella, A. T. *Angew. Chem., Int. Ed.* **1999**, *38*, 750−770.

(4) (a) Isoma, P.; Polaina, J.; Latorre-Garcia, L.; Canada, F. J.; Gonzalez, B.; Sanz-Aparicio, J. *J. Mol. Biol.* **2007**, *371*, 1204−1218. (b) Gloster, T. M.; Roberts, S.; Ducros, V. M.-A.; Perugino, G.; Rossi, M.; Hoos, R.; Moracci, M.; Vasella, A.; Davies, G. J. *Biochemistry* **2004**, *43*, 6101−6109.

(5) (a) Biarnés, X.; Nieto, J.; Planas, A.; Rovira, C. *J. Biol. Chem.* **2006**, *281*, 1432−1441. (b) Biarnes, X.; Ardevol, A.; Planas, A.; Rovira, C. *Biocatal. Biotransform.* **2010**, *28*, 33−40.

(6) (a) Deslongchamps, P. Intramolecular Strategies and Stereoelectronic Effects: Glycosides and Orthoesters Hydrolysis Revisited. In *The Anomeric Effect and Associated Stereoelectronic Effects*; Thatcher, G. R. J., Ed.; ACS Symposium Series 539: Washington, DC, 1993; pp 26−54. (b) Perrin, C. L. Anomeric Effects: An Iconoclastic View. In *The Anomeric Effect and Associated Stereoelectronic Effects*; Thatcher, G. R. J., Ed.; ACS Symposium Series 539: Washington, DC, 1993; pp 70−96. (c) Sinnott, M. L. No Kinetic Anomeric Effect in Reactions of Acetal Derivatives. In *The Anomeric Effect and Associated Stereoelectronic Effects*; Thatcher, G. R. J., Ed.; ACS Symposium Series 539: Washington, DC, 1993; pp 97−113.

(7) Cocinero, E. J.; Carcabal, P.; Vaden, T. D.; Simons, J. P.; Davis, B. G. *Nature* **2011**, *469*, 76−80.

(8) DeMatteo, M. P.; Snyder, N. L.; Morton, M.; Baldisseri, D. M.; Hadad, C. M.; Peczuh, M. W. *J. Org. Chem.* **2005**, *70*, 24−38.

(9) DeMatteo, M. P.; Mei, S.; Fenton, R.; Morton, M.; Baldisseri, D. M.; Hadad, C. M.; Peczuh, M. W. *Carbohydr. Res.* **2006**, *341*, 2927−2945.

(10) Markad, S. D.; Miller, S. M.; Morton, M.; Peczuh, M. W. *Tetrahedron Lett.* **2010**, *51*, 1209−1212.

(11) Woods, R. J.; Andrews, C. W.; Bowen, J. P. *J. Am. Chem. Soc.* **1992**, *114*, 859−864.

(12) Andrews, C. W.; Fraser-Reid, B.; Bowen, J. P. *J. Am. Chem. Soc.* **1991**, *113*, 8293−8298.

(13) Deslongchamps, P.; Li., S.; Dory, Y. L. *Org. Lett.* **2004**, *6*, 505−508.
(14) (a) van Eikeren, P. *J. Org. Chem.* **1985**, *45*, 4641−4645. (b) Deslongchamps, P.; Dory, Y. L.; Li, S. *Can. J. Chem.* **1994**, *72*, 2021−2027.
(15) Bérces, A.; Enright, G.; Nukada, T.; Whitfield, D. M. *J. Am. Chem. Soc.* **2001**, *123*, 5460−5464.
(16) Stubbs, J. M.; Marx, D. *Chem.—Eur. J.* **2005**, *11*, 2651−2659.
(17) Satoh, H.; Hansen, H. S.; Manabe, S.; van Gunsteren, W. F.; Hünenberger, P. H. *J. Chem. Theory Comput.* **2010**, *6*, 1783−1797.
(18) Namchuck, M. N.; McCarter, J. D.; Becalski, A.; Andrews, T.; Withers, S. G. *J. Am. Chem. Soc.* **2000**, *122*, 1270−1277.
(19) Mega, T.; Matsushima, Y. *J. Biochem.* **1983**, *94*, 1637−1647.
(20) Withers, S. G.; Percival, M. D.; Street, I. P. *Carbohydr. Res.* **1989**, *187*, 43−66.
(21) Withers, S. G.; MacLennan, D. J.; Street, I. P. *Carbohydr. Res.* **1986**, *154*, 127−144.
(22) Edward, J. T. *Chem. Ind.* **1955**, 1102−1104.
(23) Bennet, A.; Sinnott, M. L. *J. Am. Chem. Soc.* **1986**, *108*, 7287−7294.
(24) Sinnott, M. L.; Jencks, W. P. *J. Am. Chem. Soc.* **1980**, *102*, 2026−2032.
(25) Baker., F. W.; Parish, R. C.; Stock., L. M. *J. Am. Chem. Soc.* **1967**, *89*, 5677−5685.
(26) Capon, B. *Chem. Rev.* **1969**, *69*, 407−498 and cited references..
(27) *Molecular Operating Environment*, version 2007.09; Chemical Computing Group: Montreal, Quebec, Canada, 2007.
(28) (a) Halgren, T. A. *J. Comput. Chem.* **1996**, *17*, 490−641. (b) Halgren, T. A. *J. Comput. Chem.* **1999**, *20*, 720−729, 730−741.
(29) Frisch, M. J.; Trucks, G. W.; Schlegel, H. B.; Scuseria, G. E.; Robb, M. A.; Cheeseman, J. R.; Scalmani, G.; Barone, V.; Mennucci, B.; Petersson, G. A.; Nakatsuji, H.; Caricato, M.; Li, X.; Hratchian, H. P.; Izmaylov, A. F.; Bloino, J.; Zheng, G.; Sonnenberg, J. L.; Hada, M.; Ehara, M.; Toyota, K.; Fukuda, R.; Hasegawa, J.; Ishida, M.; Nakajima, T.; Honda, Y.; Kitao, O.; Nakai, H.; Vreven, T.; Montgomery, J. A., Jr.; Peralta, J. E.; Ogliaro, F.; Bearpark, M.; Heyd, J. J.; Brothers, E.; Kudin, K. N.; Staroverov, V. N.; Kobayashi, R.; Normand, J.; Raghavachari, K.; Rendell, A.; Burant, J. C.; Iyengar, S. S.; Tomasi, J.; Cossi, M.; Rega, N.; Millam, N. J.; Klene, M.; Knox, J. E.; Cross, J. B.; Bakken, V.; Adamo, C.; Jaramillo, J.; Gomperts, R.; Stratmann, R. E.; Yazyev, O.; Austin, A. J.; Cammi, R.; Pomelli, C.; Ochterski, J. W.; Martin, R. L.; Morokuma, K.; Zakrzewski, V. G.; Voth, G. A.; Salvador, P.; Dannenberg, J. J.; Dapprich, S.; Daniels, A. D.; Farkas, Ö.; Foresman, J. B.; Ortiz, J. V.; Cioslowski, J.; Fox, D. J. *Gaussian 09*, revision A.1; Gaussian, Inc.: Wallingford CT, 2009.
(30) (a) Becke, A. D. *J. Chem. Phys.* **1993**, *98*, 1372−1377. (b) Lee, C.; Yang, W.; Parr, R. G. *Phys. Rev. B* **1998**, *37*, 785−789.
(31) Hariharan, P. C.; Pople, J. A. *Chem. Phys. Lett.* **1972**, *16*, 217−219.
(32) Cossi, M.; Barone, V.; Cammi, R.; Tomasi, J. *Chem. Phys. Lett.* **1996**, *255*, 327−335.
(33) Marenich, A. V.; Cramer, C. J.; Truhlar, D. G. *J. Phys. Chem. B* **2009**, *113*, 6378−6396.
(34) Hratchian, H. P.; Schlegel, H. B. *J. Chem. Theory Comput.* **2005**, *1*, 61−69.
(35) National Institute of Standards and Technology, http://srdata.nist.gov/ccbdb.
(36) Zhao, Y.; Truhlar, D. G. *Theor. Chem. Acc.* **2008**, *120*, 215−241.
(37) (a) Zhao, Y.; Truhlar, D. G. *Org. Lett.* **2006**, *8*, 5753−5755. (b) Zhao, Y.; Schultz, N. E.; Truhlar, D. G. *J. Chem. Theory Comput.* **2006**, 364−382.
(38) Csonka, G. I.; French, A. D.; Johnson, G. P.; Stortz, C. A. *J. Chem. Theory Comput.* **2009**, *5*, 679−692.
(39) Cramer, C. J.; Truhlar, D. G.; French, A. D. *Carbohydr. Res.* **1997**, *298*, 1−14.